Climate Services 19 (2020) 100182

Contents lists available at ScienceDirect

Climate Services

journal homepage: www.elsevier.com/locate/cliser

Improving the seasonal prediction of Northern Australian rainfall onset to help with grazing management decisions

Tim Cowan[a,*], Roger Stone[a], Matthew C. Wheeler[b], Morwenna Griffiths[b]

[a] Centre for Applied Climate Sciences, University of Southern Queensland, Toowoomba, QLD, Australia
[b] Bureau of Meteorology, 700 Collins St, Melbourne, VIC, Australia

ARTICLE INFO

Keywords:
Seasonal prediction
Wet season onset
Calibrated forecasts
Northern Australia
Interannual variability
Northern rainfall onset

ABSTRACT

The development of the Australian Community Climate and Earth-System Simulator-Seasonal prediction system version 1 (ACCESS-S1) signifies a major step towards addressing predictive limitations in multi-week to seasonal forecasting throughout Australia. It is anticipated that moving to ACCESS-S1 will provide improved skill in rainfall prediction during the dry to wet season transition period across tropical northern Australia. This is an important time for northern Australian livestock producers in terms of the decisions they make around pasture and livestock management. This study quantifies the hindcast skill of ACCESS-S1 for the northern rainfall onset (NRO), defined as the date when 50 mm of precipitation has accumulated at a given location from the 1st of September, heralding the shift towards greener pastures. We evaluate the raw model hindcasts, and compare them to hindcasts corrected for mean biases and those calibrated against observations. It is found that the raw ACCESS-S1 hindcasts broadly replicate the observed median NRO over the period 1990–2012, despite a tendency for earlier than observed onsets. In terms of forecasting the interannual variability of the NRO, the calibrated hindcasts show the greatest skill, with the largest improvements over a climatological forecast in their probabilistic forecasts of an earlier or later than usual onset, with a large portion of northern Australian showing more than 10% improvement. With real-time NRO forecasts now generated by ACCESS-S1, it is expected that the calibrated predictions will help northern Australian graziers make better informed decisions around livestock management prior to the wet season.

Practical Implications

Across northern Australia, the large year-to-year variations in rainfall during the summer wet season (Mollah and Cook, 1996; Brown et al., 2019) creates a challenging environment for cattle and sheep producers to manage the emerging climate risk (Cobon et al., 2020). There is a pressing need for more skilful weather and seasonal forecasts, and better suited forecast products designed to help producers with seasonal management decisions around forage budgeting, calving, mustering, re-stocking, and ordering supplies that last through the wet season (Balston and English, 2009; Cobon et al., 2020). These decisions can be influenced by the onset of first decent rainfall after the dry season (Lo et al., 2007; Drosdowsky and Wheeler, 2014), the frequency and magnitude of monsoon rainfall bursts (Narsey et al., 2018), and the retreat of the monsoon (Lisonbee et al., 2019). One such forecast product tailored for northern Australian graziers is the northern rainfall onset (NRO), defined as the date when an accumulation of 50 mm of rainfall is reached after the 1st of September. Typically, northern Australia's (i.e., north of 29°S) dry season extends from May to September, with the NRO occurring from October to February, depending on location. The NRO is a proxy for the emergence of new pasture after the dry season, from which graziers can plan livestock foraging on the commencement of the wet season (McCown, 1981; McCown et al., 1981). The NRO is largely influenced by large-scale changes in the equatorial Pacific associated with the El Niño-Southern Oscillation, wherein onsets often occur later than usual for El Niño and earlier than usual for La Niña events. Operational forecasts of the NRO began in 2015 using the Australian Bureau of Meteorology's older-generation coupled dynamical model. The forecasts are issued from June each year, giving producers close to a 5–6 month window for decision planning.

This study assesses the performance of the Bureau's latest multi-week to seasonal model, ACCESS-S1, which became operational in 2018 (Hudson et al., 2017a), at both capturing the long-term observed climatology of the NRO, as well as forecasting its year-to-year variability. Tailoring forecasts products for the livestock producers of northern Australia is a key aspect of this

* Corresponding author.
E-mail address: tim.cowan@bom.gov.au (T. Cowan).

https://doi.org/10.1016/j.cliser.2020.100182

research. There has already been a successful uptake of ACCESS-S1 forecast products in fisheries (de Burgh-Day et al., 2019), in the management of the Great Barrier Reef (Smith et al., 2019) and for southern Australian horticultural regions (Hudson et al., 2017b). Yet, very few forecast products exist that are specific to graziers in northern Australia. In a practical sense, a confident forecast of an earlier than normal onset might provide the impetus for a producerto plan the rotation of their livestock to more suitable pastures. Or alternatively, a forecast of a later than normal onset may indicate to a producer that supplementary feed is required and livestock mating may need to be pushed back later in the wet season.

In this study, we show that the NRO forecast for 2019/2020 was for a later than normal onset across much of northern and eastern Australia, and this verified as a widely successful prediction, despite there being no strong climate influence in the equatorial Pacific. Through skilful forecasts like this, it is hoped that there will be a wider uptake and usage of simple forecast products like the NRO. Drawing on the local expertise of graziers, a dialogue can be created between researchers and producers on the requirements for more tailored forecast products that describe other aspects of the wet season, like monsoon bursts and breaks with rainfall thresholds altered to suit user requirements. Furthermore, there is also a push to create a forecast product describing the monsoon cessation date, which will help producers with dry season stock decisions (e.g., exporting cattle). The ultimate goal of this research is to improve producer resilience to episodic drought and other extremes by arming them with improved climate and weather information specific to their own region. Therefore, a first practical step is to provide greater community awareness of the available forecast products like the NRO to producers so that they may be incorporated into their annual management decisions.

1. Introduction

Northern Australia experiences pronounced dry and wet seasons (Pope et al., 2009; Berry and Reeder, 2016), with the time of transition (e.g., onset) from dry to wet being of great interest for climate researchers since the 1960s (Lisonbee et al., 2019). One of the first northern Australian wet season onset definitions considered was when the first wide-spread rains occurred after the 1st of November (Troup, 1961), often accompanied by low-level westerly winds. This reversal of the low-level easterlies to westerlies has historically defined the start of the Australian monsoon (McBride, 1987). In the early 1980s, wet season onset definitions were tested using different rainfall threshold values, ranging from 10 mm to 500 mm, accumulated from the 1st of August (Nicholls et al., 1982). For the northern Australian city of Darwin (see location in Fig. 2), Nicholls et al. (1982) found that for the period 1952–1980, the 50 mm accumulation threshold typically occurred around the 26th of October, leading to later work mainly focusing on a rainfall accumulation from the 1st of September (Nicholls, 1984; Lo et al., 2007).

The Australian Bureau of Meteorology (BOM) defines the date at which 50 mm of rainfall has accumulated after the 1st of September as the northern rainfall onset (NRO) (Drosdowsky and Wheeler, 2014). The simplicity of the definition means that it can be easily understood by users in the cropping and cattle grazing sectors across northern Australia. The atmospheric dynamics related to the NRO vary according to year and region. For example, for Darwin, onsets can result from short rainfall bursts over 1–2 days from localised weather systems, as was observed in 1964. In that particular year, onset was reached after only two rainfall days in early September. Alternatively, the onset can be more gradual as was the case for Darwin in 1977 where onset was reached in late November, in response to a more extensive active monsoon phase affecting the whole of the Northern Territory.

The northern Australian grazing and cropping industries use the NRO as a proxy date for the stimulation of new pasture growth across the northern tropics, similar to the 'green date' (McRae, 2013) or 'green break in the season' (Balston and English, 2009). The main difference is that green date/break definitions require relatively high rainfall accumulations over a period of less than a week (Lisonbee et al., 2019), useful for regions requiring follow-up rainfall for planting crops (Mollah and Cook, 1996) or for foraging cattle (Balston and English, 2009). Importantly, the NRO can be skilfully predicted primarily due to its strong association with the El Niño-Southern Oscillation (ENSO) (Lo et al., 2007), and as such, any improvement in a forecast systems' predictability of ENSO are likely to lead to more accurate seasonal predictions of the NRO. Its usefulness also stems from the fact that good skill in its prediction can be determined as early as June (Drosdowsky and Wheeler, 2014).

As of 2018, the BOM shifted their operational seasonal predictions over to the Australian Community Climate and Earth-System Simulator-Seasonal prediction system version 1; or ACCESS-S1 (Hudson et al., 2017a). Prior to this, the BOM were publicly providing three seasonal probabilistic forecasts of the NRO per year, released towards the end of June, July and August, using an older-generation coupled system: the Predictive Ocean–Atmosphere Model for Australia version 2 (POAMA2). A previous verification study by Drosdowsky and Wheeler (2014) showed that POAMA2 is particularly skilful in predicting the NRO relative to its own long-term median in 50-year hindcasts, with the greatest predictability over the Northern Territory. The Drosdowsky and Wheeler (2014) study showed a reduction in POAMA2's skill during neutral or weak ENSO years, and noted the model's dry bias, hence the reason to compare against POAMA's long-term NRO median. Despite this, the probabilistic skill of POAMA2 was found to be higher than that from a statistical forecast using the relationship between the NRO and the austral winter Southern Oscillation index (SOI) (Lo et al., 2007). Higher frequency subseasonal modes of variability like the Madden-Julian Oscillation (MJO) show improved subseasonal prediction in ACCESS-S1 compared to POAMA2 (Marshall and Hendon, 2019), however given the MJO can only be skilfully forecast out to 25 days in summer, it does not assist in the predictability of the NRO given the 1 September forecast cut-off. It is likely that MJO activity in the model hindcasts does lead to onsets over many locations, however these cannot be skilfully predicted at the seasonal time-scale. It has been shown that ACCESS-S1 has better skill in forecasting mean-state temperatures and rainfall across Australia than POAMA2 (Shi et al., 2016; Hudson et al., 2017b), even though it features a large summer wet bias (> 0.5 mm/day) across central Australia (Fig. S1 in Supplementary Material). Hence this study's main aim is to verify the skill of ACCESS-S1's hindcasts with respect to the NRO, and, in doing so, determine if there is discernible improvement over POAMA2. We first quantify the observed long-term median NRO and then assess the representation of this in ACCESS-S1 (i.e., does it simulate the spatial variability across northern Australia?). In the context of the ACCESS-S1 evaluation, we investigate whether there is skill improvement when the raw hindcasts are separately bias corrected and calibrated to the finer scale resolution of the observations.

2. Data and methods

2.1. Observations

For this study, we use observed high-resolution (5 km) gridded daily rainfall from the Australian Water Availability Project (Jones et al., 2009; AWAP), using data since 1960 in line with the Drosdowsky and Wheeler (2014) study. Given the northern Australia focus, we only use land points north of 29°S (see Fig. 1), an area that stretches from the Queensland/New South Wales border to Cape York in the far northeast and west to the Pilbara-Gascoyne Basin; it includes the major livestock grazing regions of the Gulf of Carpentaria, the Northeast Coast and the Tanami-Timor Sea Coast. In regions encompassing the North Western

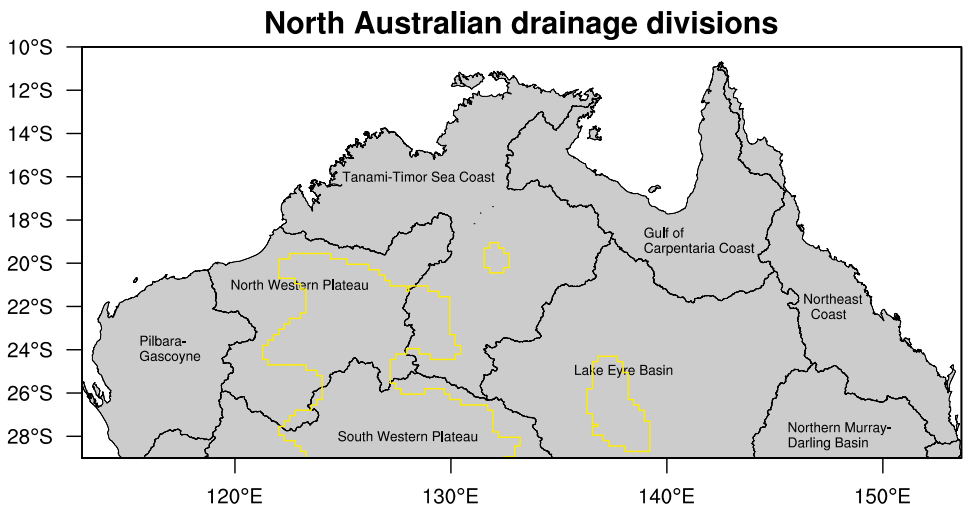

Fig. 1. Major drainage regions of northern Australia. These regions are referred to throughout the study. Also shown are the regions in yellow where there is insufficient station density.

and South Western Plateaus and smaller areas of the Lake Eyre Basin and Tanami-Timor Sea Coast, the observational station density is insufficient for determining the NRO on a daily temporal scale and hence has been masked out (yellow regions in Fig. 1). This mask is applied to the same regions for the hindcasts and does not change across the hindcast period. After calculating the observed median NRO, we apply a 1-2-1 spatial filter 50 times latitudinally and longitudinally to smooth out local inconsistencies (Lo et al., 2007). We arbitrarily choose 50 applications of the filter to better fit with previously displayed NRO patterns using the 1° AWAP product (Drosdowsky and Wheeler, 2014). It has also been shown that spatial smoothing improves the skill of a statistical forecast of the NRO (Lo et al., 2007).

2.2. ACCESS-S1 description

ACCESS-S1 is the BOM's newest coupled seasonal prediction system, and became operational in 2018, replacing POAMA2 (Hudson et al., 2017a). The atmospheric component is based on the UK Met Office's Global Coupled model configuration 2 forecast system (MacLachlan et al., 2015), with a N216 (60 km in the mid-latitudes) horizontal resolution and 85 vertical levels, while the land surface model is the Joint UK Land Environment Simulator with four soil levels (Walters et al., 2017). In comparison, POAMA2's horizontal resolution is approximately 250 km with 17 vertical levels (Hudson et al., 2013). The ocean component of ACCESS-S1 has a 0.25° horizontal resolution on a tripolar grid with 75 levels in the vertical, and it relies on the Met Office's Forecast Ocean Assimilation Model for its ocean and sea-ice initial conditions. The atmosphere and land temperature components are initialised by ECMWF Re-Analysis(ERA)-Interim (Dee et al., 2011), interpolated onto the N216 grid (Hudson et al., 2017a). The ACCESS-S1 prediction system includes important climate and weather modes of variability (e.g., ENSO, MJO), as well as synoptic-scale weather systems and oceanic eddies, which allows the BOM to provide a probabilistic prediction service from the weekly to seasonal time-frame.

2.3. ACCESS-S1 hindcasts

The ACCESS-S1 hindcasts consist of an ensemble of 11 members run for 217 days from a set of initialisation dates for each year over the period 1990–2012. The hindcasts have been initialised on the 1st, 9th, 17th and 25th of each month, however given the NRO typically occurs between October and March (i.e., austral summer), we only analyse hindcasts from 1 May through to 1 September. For example, a 1 May initialised hindcast finishes 217 days later in early December, while a 1 July initialised hindcast finishes in early February. If an onset is not reached at a given location by the end of the hindcast, then it is set to a special "no onset" value, which is determined to be either:

- a late onset if the observed median onset occurs before the end of the hindcast, meaning the "no onset" value can be used for the hindcast probability calculation; or
- an unknown onset, if the observed median onset is later than the end of the hindcast run, meaning this "no onset" value cannot be included in the hindcast probability.

To sample uncertainty in the initial conditions, a scaled perturbation was introduced into each ensemble member's atmospheric state based on randomly sampled 7-day differences for the month in question from ERA-Interim reanalysis over 1981–2010 (Lim et al., 2016). For this study, given the small ensemble size of 11 members and the relatively short hindcast period of 23 years, we combine three consecutive initialisation dates to create 33-member ensembles with which to calculate probabilities and skill scores. This was not required for POAMA2 given it featured 30 and 33 members for the multi-week and seasonal hindcasts, respectively (Drosdowsky and Wheeler, 2014).

Three different hindcast products are produced separately from the raw 60 km ACCESS-S1 hindcast output (for precipitation). The first product is regridded to the observed 5 km grid using a bilinear interpolation. The second product, also interpolated to a 5 km grid, is produced by mean bias-correcting the raw model output against the observations using an 11-day window. Following the bias correction, where precipitation < 0, it is set to 0. The third 5 km product is created through a quantile–quantile calibration matching technique (Jeon et al., 2016), which is applied to all locations, start dates and lead times. Where the raw hindcast output falls outside the observed value, the calibrated value is calculated as the raw value × (observed max [min]/model max [min]). Further details on ACCESS-S1 data assimilation and its mean-state biases are detailed in Hudson et al., 2017a.

3. Results

3.1. Observed onset climatology

A visual representation of the NRO definition is provided in Fig. 2, showing the observed onset date for Darwin and across the Top End in 1974. The onset in Darwin for that year was reached on 3 October after three separate multi-day rainfall events on 5–7 September, 24–26 September and 1–6 October. The long-term (1960–2012) median onset

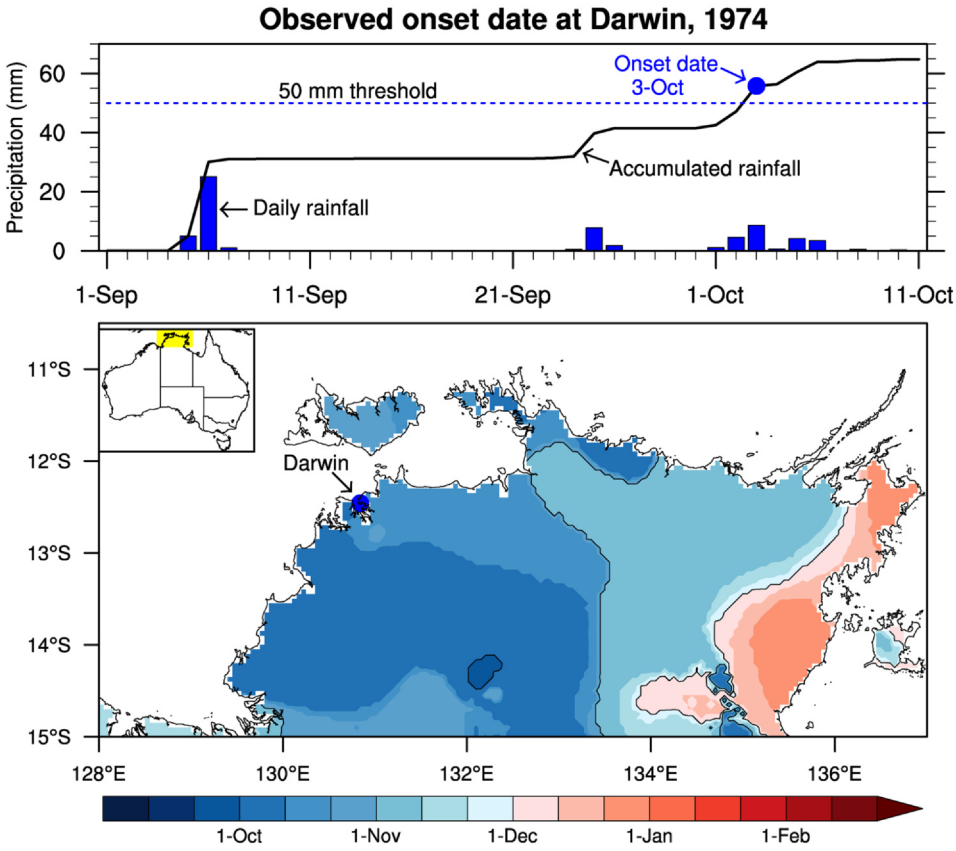

Fig. 2. (Top) Daily (blue bars) and accumulated daily rainfall (black curve) at Darwin (blue dot, lower panel), the capital city of the Northern Territory, showing the observed onset date for 1974. (Bottom) Map of onset dates across the Top End (yellow inset region) for 1974. No spatial smoothing has been applied.

date for Darwin Airport (i.e., the nearest AWAP data grid point to 12.42°S, 130.89°E) is 24 October, two days before the mean onset date using the 50 mm threshold definition of Nicholls et al. (1982) based on station data from 1952 to 1980. The onset in 1974 occurred in early October for much of the western Top End, with a clear zonal gradient of early to late (in terms of calendar month) onset from west to east, with the onset over eastern region of Arnhem Land occurring in late December.

Across the observational record, the first meaningful wide-spread rains for Darwin and the Top End typically arrive in late October, as indicated by the median NRO (Fig. 3a,c). Across the 1960–2012 period, the onset distribution for Darwin is characteristically Gaussian and quite narrow (Fig. 3c), with only one onset in the 53-year record later than mid-November. The onset expands southward through November, reaching towns like Longreach (Queensland) and Halls Creek (Western Australia) around early December. Given these inland locations display greater interannual rainfall variability (Drosdowsky and Wheeler, 2014), their onset distributions are substantially broader than for Darwin, with a slight bimodal structure. The October onsets in the eastern Northern Murray-Darling Basin and along the far Northeast Coast stem from the fact that rainfall can occur there any time during the austral winter and spring months (Drosdowsky and Wheeler, 2014). By January, the onset reaches the southern Lake Eyre Basin and the western parts of the North Western Plateau, before spreading to the Pilbara-Gascoyne by February. As in Lo et al. (2007) and Drosdowsky and Wheeler (2014), we apply a 1-2-1 (3-point) spatial filter to the median pattern (Fig. 3b). This reduces the spatial noise of the 5 km observed NRO, but preserves the large-scale spatial gradients.

Earlier or later than median NRO can indicate a greater likelihood of a strong or weak wet season, particularly in years featuring El Niño or La Niña events (Lo et al., 2007). Fig. 4 shows a comparison between the median NRO and austral late spring to early summer (October to January) rainfall for all El Niño and La Niña years over the 1960–2012 period. The ENSO years are based on the July to August SOI values exceeding −8.0 (El Niño) or 8.0 (La Niña; years are listed in the Fig. 4 caption), and refer to the year that December falls in. During El Niño years, the late spring to early summers have a tendency for wide-spread negative rainfall anomalies of −1.5 mm/day across Cape York; elsewhere, anomalies of between 0 and −0.5 mm/day are observed (Fig. 4b). These patterns are reflected in the NRO, with later onsets across the western Top End (early November) and across the Gulf of Carpentaria (late November to early December; Fig. 4a). For La Niña years, most of far northern Australia experiences positive late spring to early summer rainfall anomalies exceeding 0.5 mm/day (Fig. 4d), and earlier than median onsets across most regions. These include October onsets along the Tanami-Timor Sea Coast and late September onsets across far eastern Queensland (Fig. 4c), while Pilbara-Gascoyne onsets occur ~1 month earlier (in late December) compared to onsets during El Niño years. Around 64% of all cases are ENSO neutral years, with previous research showing a general lack of skill in predicting the NRO during weak ENSO years (Drosdowsky and Wheeler, 2014). This could translate into reduced skill in predicting wet season rainfall, which may be offset by improvements in ACCESS-S1's overall prediction of ENSO (compared to POAMA2) in its build-up phase during austral autumn (Hudson et al., 2017a). It is also worth noting that the hindcast period is dominated by a number of strong La Niña events and negative Inter-decadal Pacific Oscillation conditions. ACCESS-S1 has been shown to have more accurate forecasts of spring and summer rainfall during La Niña events than during other seasons, which reflects an over-confidence in the ACCESS-S1 hindcasts (King et al., 2019).

3.2. Hindcast onset climatology

To evaluate the performance of ACCESS-S1 hindcasts in capturing

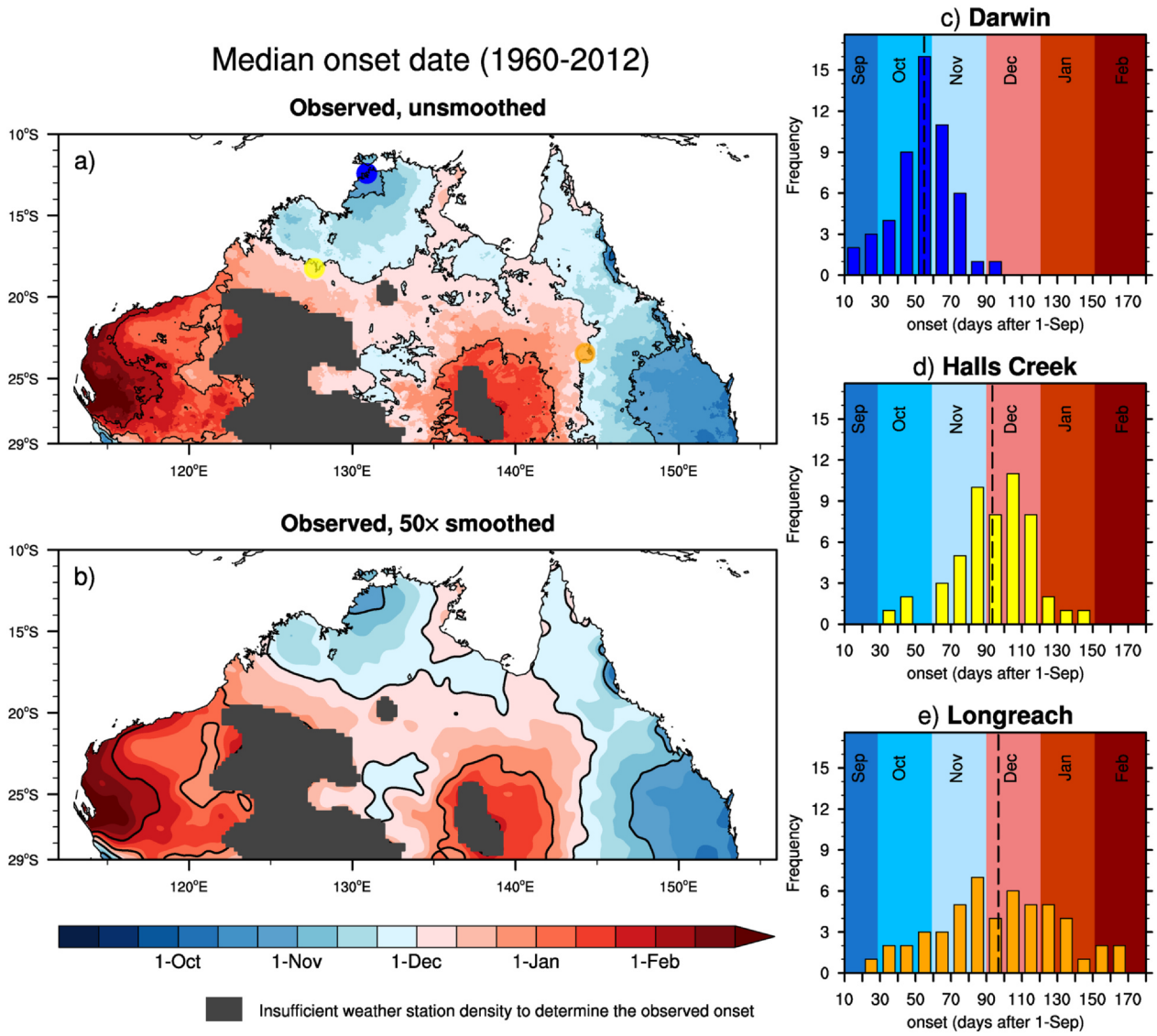

Fig. 3. Observed median northern rainfall onset dates over 1960–2012 based on (a) unsmoothed data, and (b) data smoothed 50× using a 1-2-1 spatial filter. Coloured dots indicate the locations shown in the right hand side panels, that are the distribution of the onsets for (c) Darwin, (d) Halls Creek, and (e) Longreach, as well as their medians (dashed vertical line). The map contour lines indicate the first day of each month. Dark grey shading represents regions where weather station density is insufficient for the northern rainfall onset calculation.

the spatial variability of the observed NRO, we first determine the observed median onset over the period 1990–2012 to match the hindcast period (Fig. 5a). For the ACCESS-S1 hindcasts, the median NRO is calculated from the 11-member ensemble initialised on 1 September. The results show the raw ACCESS-S1 hindcast ensemble, regridded to a 5 km resolution, broadly reproduces the western Top End and southeast Queensland onset climatology (Fig. 5b). However, a number of deficiencies exist; these include early onset biases over the northern tip of Cape York (far Northeast Coast), much of the interior and Pilbara-Gascoyne. In general, the raw regridded hindcast ensemble reproduces the large-scale southwest gradients from the Top End to the Pilbara-Gascoyne, but fails to replicate the later onsets that stretch inland from the Gulf of Carpentaria to the northern Lake Eyre Basin. The hindcast onset climatology pattern also shows predominantly November onsets across the Lake Eyre Basin, when in reality the observed onsets occur well into December and January. The regridded hindcast pattern also does not feature the localised October onset between the Northeast Coast regional cities of Cairns and Townsville and other finer-scale spatial maxima, which may reflect ACCESS-S1's coarse resolution.

Bias correcting improves the hindcast representation of onsets along the east coast, most notably around Cairns and Townsville, while also capturing the zonal gradient inland from southeast Queensland (Fig. 5c). Yet despite these improvements with more finer-scale spatial detail than the purely regridded hindcasts, the bias corrected ensemble generates onset biases of ~10–20 days earlier than observed over the northern Lake Eyre Basin. Furthermore, the bias corrected ensemble fails to generate the meridional gradient from the southern Top End through to the Tanami-Timor Sea Coast. Of the three hindcast sets, the calibrated ensemble performs the best, including capturing the late February onset over the western Pilbara-Gascoyne (Fig. 5d). The calibrated ensemble also displays the large-scale gradients and observed spatial distribution not seen in the raw regridded or bias corrected ensembles; these include the later onsets over the Lake Eyre Basin, east Arnhem Land and the zonal band between 19°-23°S.

To highlight the differences in spatial gradients between the climatological median onsets over 1990–2012 from the hindcast ensembles and observations, Fig. 6 compares the three hindcast sets over four important cattle regions. In each panel, a single dot represents the climatological median onset day from observations and the hindcast ensemble (1 September initialisation) for a given grid point in the

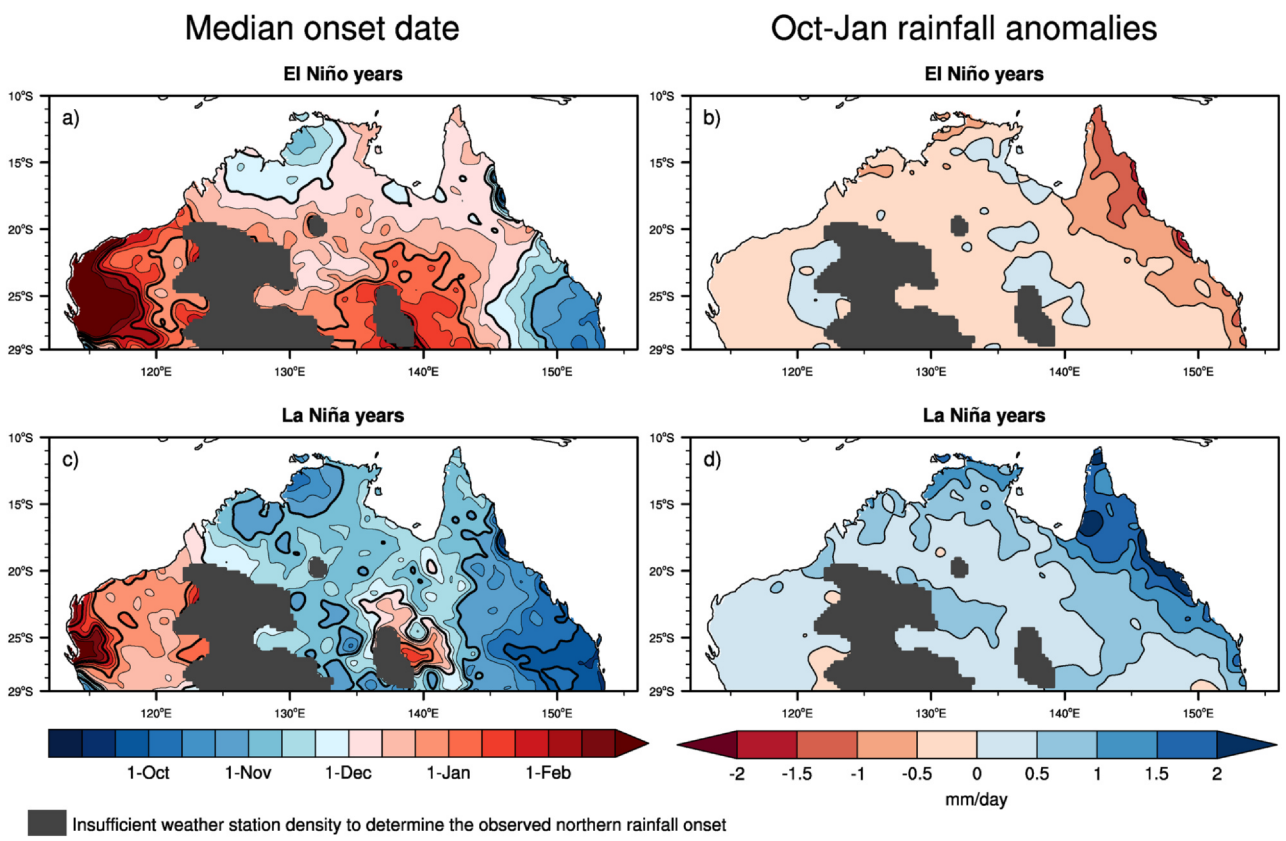

Fig. 4. (a,c) Observed median northern rainfall onset dates, and (b,d) October-January rainfall anomalies for (a,b) El Niño years (July-August SOI < −8; 1965, 1972, 1976–77, 1982, 1987, 1993–94, 1997, 2002, 2006), and (c,d) La Niña years (July-August SOI > +8; 1964, 1971, 1973–75, 1988, 1998, 2010). Contour lines indicate the first day of each month. Rainfall anomalies are calculated with respect to a 1960–2012 climatology. Dark grey shading represents regions where weather station density is insufficient for the northern rainfall onset calculation, and has been applied to all panels. All maps have been smoothed 50× using a 1-2-1 spatial smoother.

region of interest; this produces scatterplots consisting of between 7575 points for the Top End to over 10,100 points for southeast Queensland (regions are shown in Fig. 6). This provides a simple way of comparing the hindcast spatial distribution of the climatological median onset across each region with the observed onset. For the Halls Creek region (red box, Fig. 6), the raw regridded hindcast shows difficulty in reproducing climatological onsets that exceed 100 days (i.e., December onsets), which are a feature in the south of the region (Fig. 3). This problem is marginally improved through bias correction and vastly improved after calibration, particularly for later onset dates. Over the Top End (grey box, Fig. 6), the raw regridded climatological onsets occur around 30 days earlier than observations which reduces to 15–20 days earlier for the model onsets > 80 days (late November). This reflects the raw hindcast's inability to realistically represent the zonal gradient in onsets across the Top End, notably throughout Arnhem Land. This is substantially improved through bias correction, while further improvements seen in the calibrated product, particularly over east Arnhem Land, reduces the spatial disparity to the observations. The region encompassing Mount Isa and Cloncurry (orange box, Fig. 6) is where the raw hindcast ensemble performs the worst (of the four regions), with an inability to reproduce climatological onsets past early December. Bias correcting does little to improve the spatial distribution, however there is significant improvement after calibration, particularly for grid points with onsets after December. In a region like southeast Queensland where biases are not as large (blue box, Fig. 6), bias correcting improves the onsets where the climatological value is later than observed, although there is still a tendency for the model to predict earlier than observed onsets. Again, as with the other regions in Fig. 6, calibration appears to be more successful in reducing the magnitude at points displaying earlier than observed onset. This evaluation shows that calibrating the model output is the better of the two bias-correcting techniques, especially for locations that have onset dates beyond December.

3.3. Hindcast probabilities

The approach in determining the skill of the ACCESS-S1 hindcasts, with respect to the NRO, is to verify them in a probabilistic framework. To this end, we calculate the probability of an early onset for each year from 1990–2012 with respect to the (smoothed) observed 1960–2012 median for each initialisation date (1, 9, 17 and 25 of each month; May to 1 September). To increase our hindcast ensemble size, we combine three initialisation dates to form a 33 member ensemble (e.g., 9, 17, 25 of each month). We use the cross-validation approach where the hindcast probabilities are calculated with respect to an observed median NRO that does not include the year being predicted (Lo et al., 2007). In this approach we use the linear interpolation method when determining the median for an even number of years. The 'earlier than long-term median onset probability' is determined as the percentage of the 33 ensemble members that have an onset earlier than the observed median. As detailed prior, if a hindcast onset for a particular year is not reached but the observed median date precedes the date of the hindcast run end, then that onset is considered late. Hindcast onsets that fall on the median date are split evenly between the early and late categories. For comparing onset probabilities to observed onsets, we consider the observed onset anomaly to be the difference between the observed median onset and the onset of the year in question.

As an example of how the hindcast skill changes for different lead times, we show the probabilities of early than median onset for 1997 and 2002, the two strongest El-Niño years, and 1998 and 2010, the two

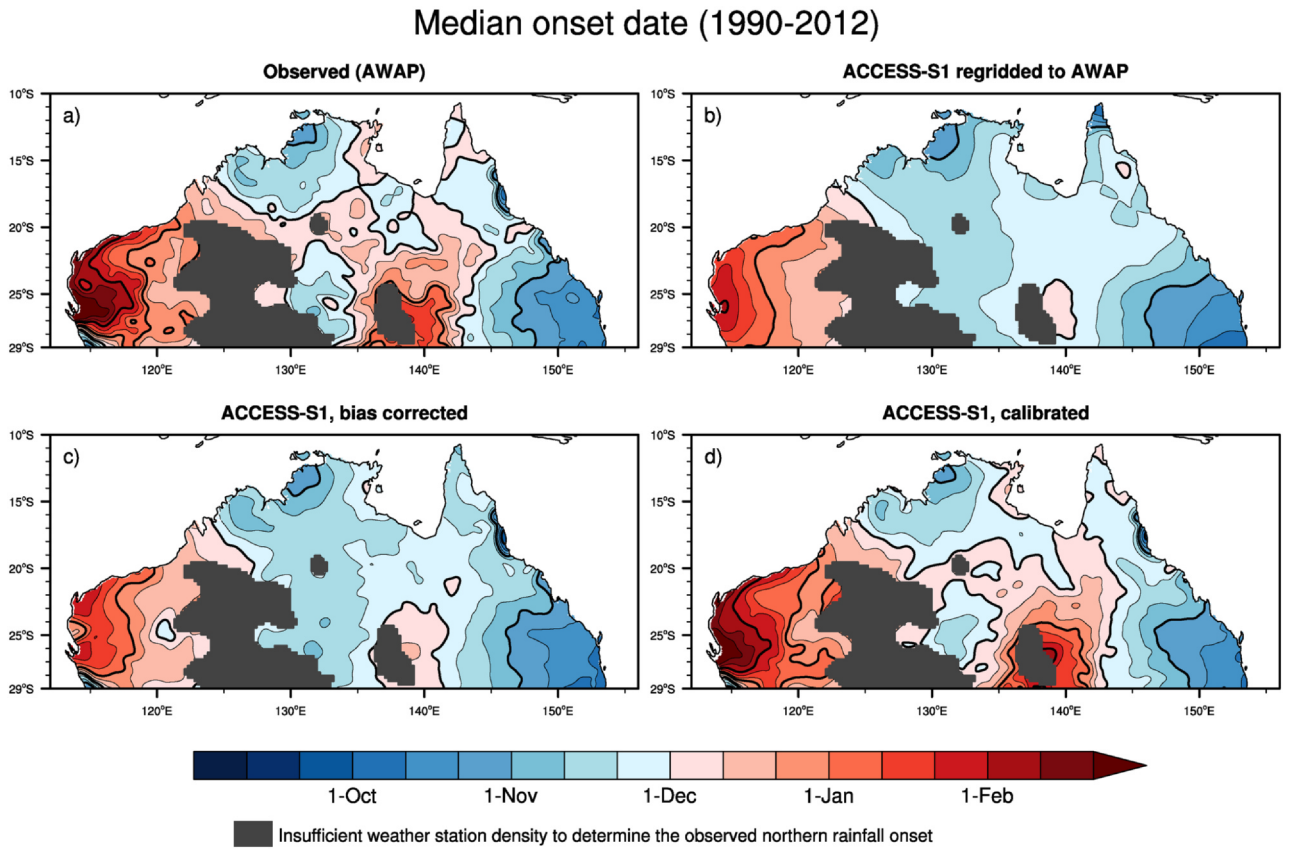

Fig. 5. Median northern rainfall onset dates over 1990–2012 for (a) observations, and ACCESS-S1 ensembles, including (b) raw model output regridded to the observed resolution, (c) bias corrected, and (d) calibrated. The ensembles are all initialised from 1 September. Details of the calibration and bias correction technique can be found in the Methods section. All maps have been smoothed 50× using a 1–2-1 spatial smoother.

strongest La Niña years (Figs. 7 and 8, respectively) for lead month 3 (9, 17, 25 May) and lead month 0 (9, 17, 25 August). Here, we are only showing the calibrated hindcasts. For 1997, the hindcast ensemble predicts little change to the onset probability from lead month 3 to 0, with a high likelihood of a later then median onset predicted over the Top End, Arnhem Land, Cape York and down the Northeast Coast, and a greater than 50% probability of early onset over central Australia (Fig. 7a,b). This generally matches the pattern of observed onset deviations, with anomalies of up to 20 days later along the Northeast Coast (Fig. 7c), reflecting the region with the strongest ENSO teleconnection in the austral spring season (Risbey et al., 2009). The model also correctly predicts a higher likelihood of early onset over central Australia, borne out in the observations. It is perhaps not unsurprising that the hindcasts are inconsistent with the very late observed onset anomalies over the Pilbara-Gascoyne region given its climatological onset falls well into February, six months after the lead month 0 hindcast. Generally, the model hindcasts also perform well in 2002 (a central Pacific El-Niño year), broadly capturing the widespread later than median onsets over north and eastern Australia, offering good predictability that does not dramatically change from lead months 3 to 0 (Fig. 7d–f).

For the La Niña years of 1998 and 2010, the model forecasts of early onset are ubiquitous across the northeast, with good predictive capability 3 months out, with probabilities exceeding 80% across central Queensland (Fig. 8). The La Niña examples suggest that the model has good predictability leading into the extremely wet monsoon seasons when the western Pacific sea surface temperature anomalies are anomalously warm and the SOI is strongly positive. This is despite ACCESS-S1's ENSO teleconnection with rainfall over Australia's east coast being weaker than observed (Hudson et al., 2017a), which may reduce predictability at longer lead times. Even for weaker La-Niña years (e.g., 1999/00, 2008/09), the hindcast probabilities show good predictability of the observed earlier than median onsets for northern Australian latitudes (see Fig. S2 in Supplementary Material). This is also consistent with the higher skill in ACCESS-S1's ENSO prediction compared to POAMA2 (Lim et al., 2016; Hudson et al., 2017a). The fact that the model hindcasts cover a period that feature strong La Niña events and negative Interdecadal Pacific Oscillation conditions infers that there is potentially an overstatement of skill in the ACCESS-S1 hindcasts (King et al., 2019). Unfortunately, the skill for the pre-1990 La-Niña wet periods of the early 1970s cannot be tested in this seasonal prediction system.

3.4. Hindcast skill

The prediction skill of ACCESS-S1 hindcasts are assessed using the Brier Skill score and reliability diagrams. The Brier Skill score quantifies the improvement of a probabilistic forecast ensemble when compared against a reference forecast (Lo et al., 2007). Here we show the improvement over a climatological forecast. The reliability diagrams demonstrate the performance of the hindcasts against the observed frequency of a given outcome for every northern Australian grid-point (Drosdowsky and Wheeler, 2014). They are used for testing if a forecast is more likely to over or under-predict the low and high probabilities of a given outcome, in this case, earlier than median onset across all Australian gridpoints north of 29°S. Here we also include an assessment of the hindcasts tercile probabilities (i.e., whether the predicted onset falls in the lowest, middle or highest third of all onsets), although in the reliability diagrams, we only show the lowest terciles (earliest onsets). As with the probabilities, three different initialisation dates are combined, where 9, 17, and 25 August represent lead month 0.

The hindcast skill scores for the early or later than median onsets for

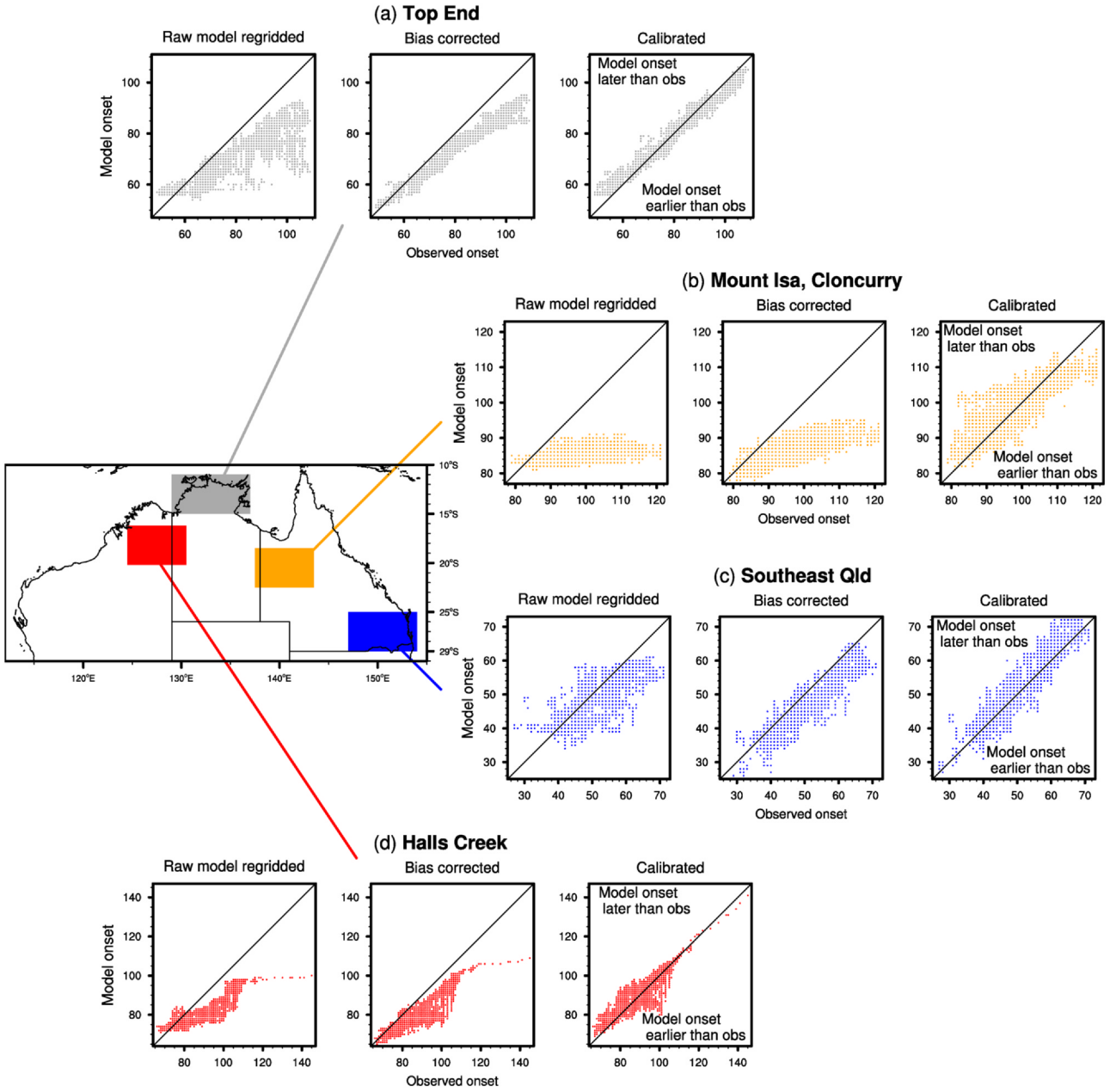

Fig. 6. A comparison of the climatological median northern rainfall onset in observations and the three ACCESS-S1 ensembles for four regions across northern Australia, including (a) Top End (grey; 129°–137°E, 11°–15°S), (b) Mount Isa and Cloncurry (orange; 137.5°–143.5°E, 18.5°–22.5°S), (c) Southeast Queensland (blue; 147°–154°E, 25°–29°S), and (d) Halls Creek (red; 124.5°–130.5°E, 16.2°–20.2°S). Each dot represents a 0.05° by 0.05° grid point in the region of interest showing the median onset from observations (x-axis) and median onset from the hindcast ensemble (y-axis) over the 1990–2012 period. The number of land-only points in each scatterplot panel range from 7575 to 10,124 points, depending on the size of the region. The initialisation date of the model ensemble members is 1 September and the axes units are days from 1 September.

each hindcast set are presented in Fig. 9. The first feature to note are the high skill scores along sections of eastern Australia, northeast Queensland and Top End in the raw regridded product (scores > 25%), which only slightly improve with shorter lead times (Fig. 9a-c). Regions of reduced skill (pink colours) are located over central Australia and the far north Cape York, consistent with the early biases in median onset pattern (Fig. 5b). There is little evidence to suggest that bias correcting improves the hindcast skill, with a large swathe of northern inland Australia indicating poorer skill (Fig. 9d–f); only small pockets including the Top End and the tip of Cape York show any marginal skill improvements, consistent with the median results (Fig. 5c). Like in their representation of the median NRO, the calibrated hindcasts are the most skilful, with nearly all inland regions that are south of 15°S and east of 132°E displaying improvements exceeding 10% over a climatology forecast (Fig. 9g–i). The percentage of northern Australia grid points that show a 10% or more improvement sits between 36% (lead month 2) and 54% (lead month 0) for the calibrated hindcasts, considerably higher than the raw and bias corrected hindcasts. This is confirmed by the reliability diagrams, with the calibrated hindcasts correcting the ACCESS-S1's over-forecasting of higher probabilities seen in the raw and bias corrected hindcasts (Fig. 10a-c).

For the tercile hindcast skill of the raw and bias corrected hindcasts, aside for eastern Queensland and the Top End, we see that most northern regions show no improvement over climatology (Fig. 11a–f). In fact, the bias correcting hindcasts show a reduction in the overall number of locations with a skill improvement greater than 10%. Again,

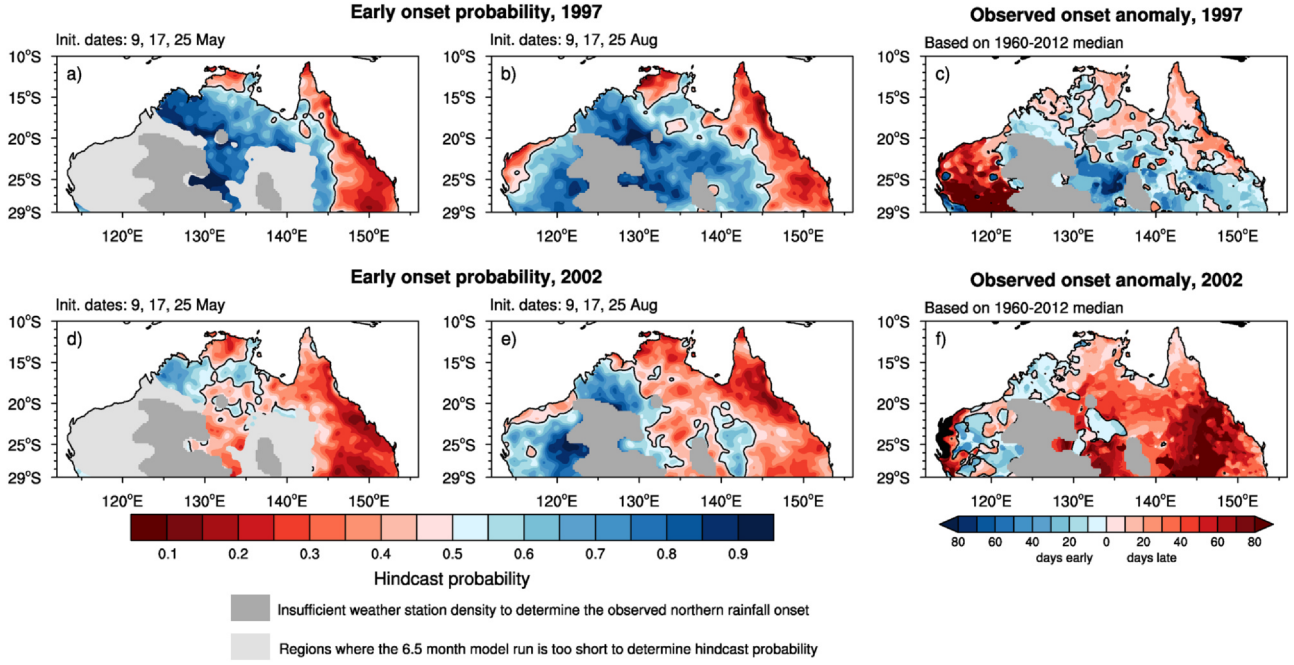

Fig. 7. Hindcast probabilities of northern rainfall onset from the calibrated ACCESS-S1 ensemble for El Niño years: (top) 1997 and (bottom) 2002, for lead months (a,d) 3 and (b,e) 0, compared to the (c,f) observed onset anomaly. Each lead month is comprised of three initialisation dates (9, 17, 25) to increase the sample size. The hindcast probabilities are calculated with respect to the observed 1960–2012 median onset that excludes the year in question in its median (cross-validation technique).

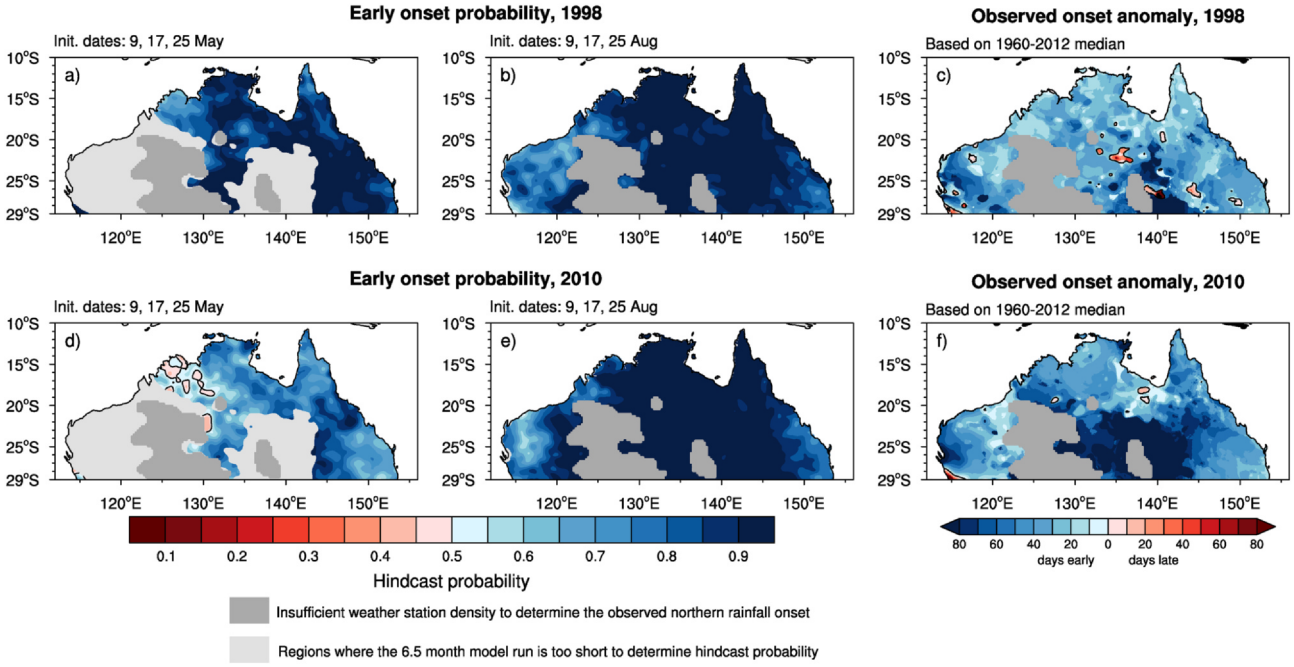

Fig. 8. As in Fig. 7, but for La Niña years 1998 and 2010.

the calibrated product provides the greatest skill, with 18% of northern Australia displaying score values exceeding 10% in lead month 2 (i.e., June) (Fig. 11g); this improvement spreads over much of northern Australia for the shorter lead months, with only the Pilbara-Gascoyne showing consistent poor skill scores (Fig. 11h,i). As with the Brier Skill Score patterns, the reliability diagrams showing the early/late onset relative to the early tercile, demonstrate the improvement in skill that calibration achieves, correcting for the over-forecasts in the higher probability bins (i.e., probabilities > 0.6; Fig. 10d–f). As expected, the raw and bias corrected hindcasts perform the most poorly in the regions where they are unable to reproduce the climatological median onsets. This produces an east-to-west gradient of reduced skill. The reasons for the poorer skill over the northwest regions relate to a weak teleconnection with remote sea surface temperatures and the general lack of a teleconnection with ENSO (Hudson et al., 2017a). Also there is the reduced skill in ACCESS-S1's prediction of weather events and extreme rainfall at longer lead times past a month (King et al., 2020) or even a fortnight, as seen in the prediction of the northern Queensland floods in February 2019 (Cowan et al., 2019). For the regions like northern-central Australia with the poorest skill, this may simply be a reflection

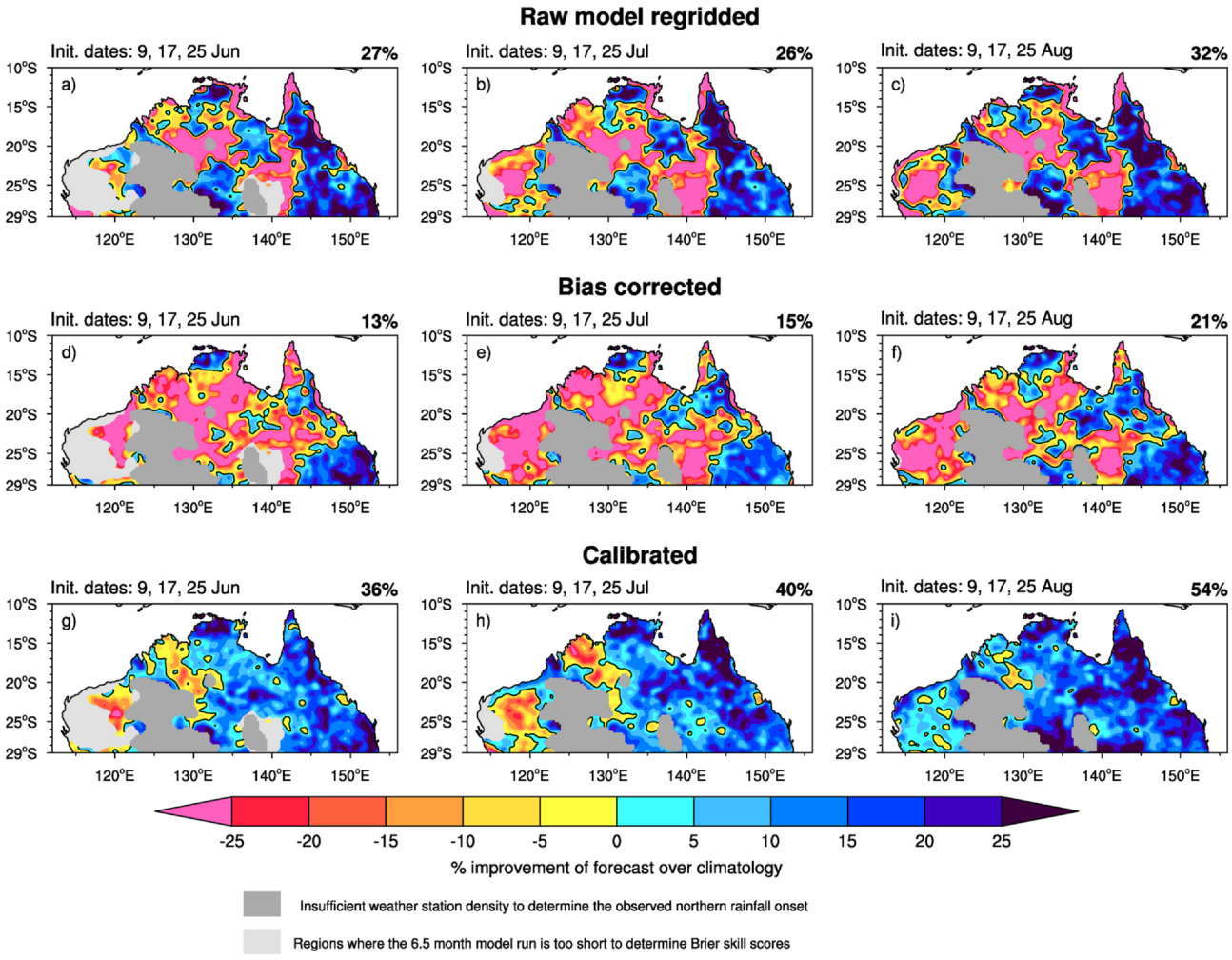

Fig. 9. Grid point Brier skill score values of the ACCESS-S1 cross-validated hindcasts of earlier or later than median onsets, relative to a climatological forecast, showing (top panels) the raw model ensemble regridded to the observed grid, (middle panels) the bias corrected ensemble, and (bottom panels) the calibrated ensemble. Combined initialisation dates include 9, 17 and 25 of June, July and August (i.e., lead months 2 to 0), respectively. In the top right corner of each panel is the percentage of grid points that show an improvement of greater than 10% over climatology.

of the acute difficulty in predicting daily rainfall and weather events almost half a year in advance. For example, the onset over central Australia occurs around mid-December, meaning a June forecast is a 6 month weather event prediction, and calibration or bias correcting cannot improve this. Across the far northern tropics, multi-day rainfall events are often associated with monsoon bursts (Berry and Reeder, 2016; Moise et al., 2019), which are difficult to forecast accurately beyond 25–30 days (Marshall and Hendon, 2019) – this is the limit of predictability of intraseasonal modes of variability like the MJO in ACCESS-S1 (Hudson et al., 2017a).

4. Discussion

This study follows on from the research of Lo et al. (2007) and Drosdowsky and Wheeler (2014), who both assessed the predictability of NRO, from a purely statistical ENSO-based standpoint in the former and using the POAMA2 dynamical model in the latter. We have continued this line of research by investigating the ability of the BOM's newest seasonal forecast system, ACCESS-S1, to predict the NRO. This study provides the verification groundwork accompanying the real-time ACCESS-S1 NRO forecasts that commenced in July 2019. The main aim here was to gauge the improvement in reliability of NRO forecasts, where the NRO marks the transition from the dry to wet season across northern Australia. Improving the NRO predictions helps end users, like northern cattle producers, make smarter and more reliable decisions around mustering, calving and feed budgeting for when the break of the season occurs (McRae, 2013). It is worth reiterating that the NRO does not represent the temporal extent or intensity of the wet season, the latter of which is more strongly linked to monsoon bursts, quasi-stationary tropical depressions and cyclones. Yet, as we have shown, the NRO displays a strong association with ENSO variability, such that from June onward, the tropical Pacific is often a useful predictor of the NRO (Lo et al., 2007), particularly over the Northeast Coast.

Despite the short temporal hindcast length of 23-years, ACCESS-S1 has the ability to reproduce the long-term median NRO across northern Australia. The regions where the model has difficulty capturing the spatial gradients include the grazing regions over inland Queensland and the Northern Territory that display onset variability of between 40 and 60 days (Drosdowsky and Wheeler, 2014). These deficiencies allow us to validate the efficacy of bias correction and calibration of the raw model hindcasts. While bias-correcting precipitation alleviates some of the November to December onset biases over Arnhem Land and across the northwest, calibrating the rainfall produces results that are closer to observations. This is because the calibration process predominantly fixes the early onset bias seen in the ACCESS-S1 hindcasts, as it accounts for biases in the mean and corrects any heavily skewed precipitation days.

Calibration also improves the skill in predicting interannual onset

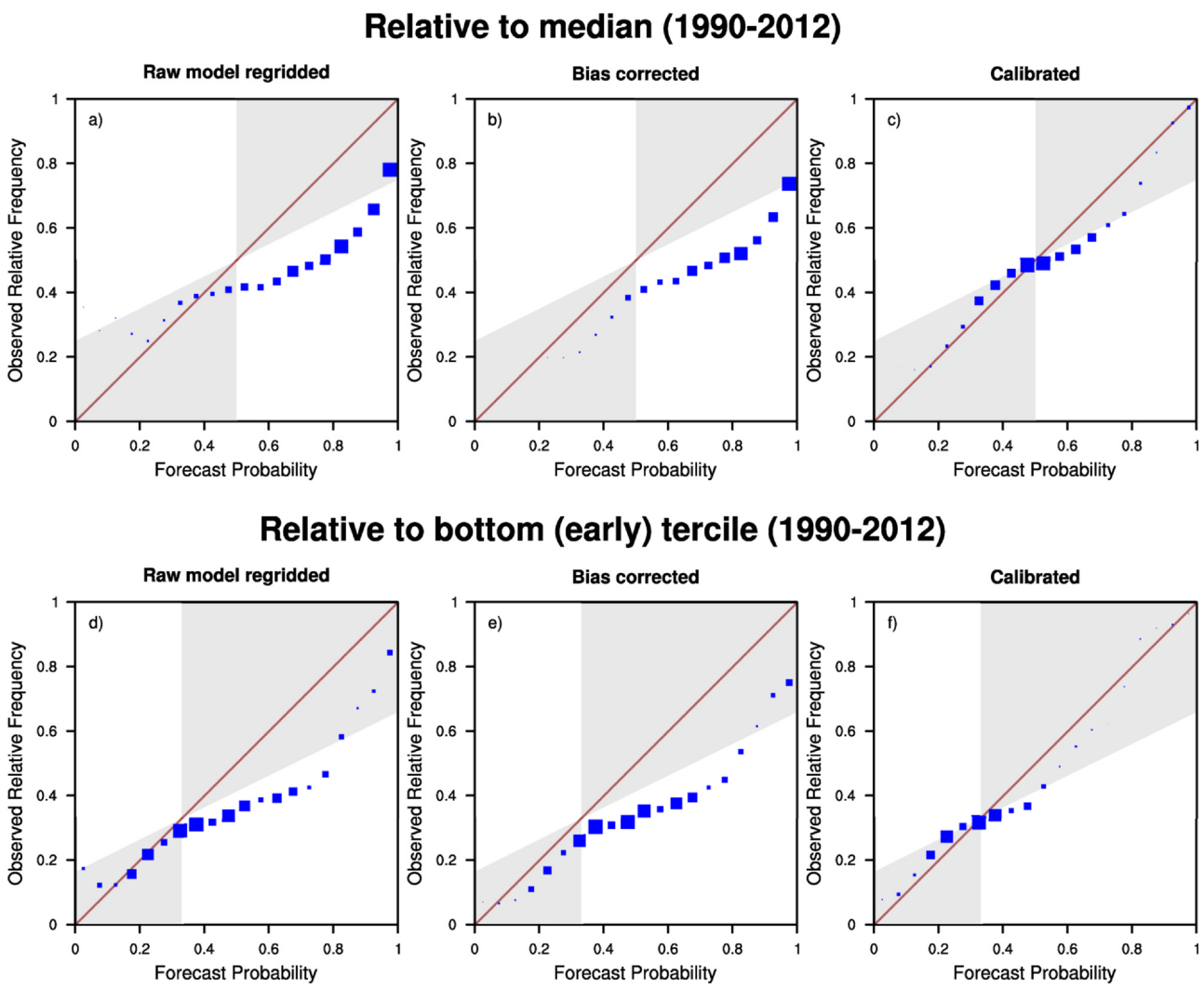

Fig. 10. Reliability diagrams showing all grid points north of 29°S for (a–c) early or late onset relative to the median onset and (d-f) early or late onset relative to the bottom (early) tercile, showing (a,d) raw model ensemble regridded to the observed grid, (b,e) the bias corrected ensemble, (c,f) the calibrated ensemble, for lead month 0 (i.e., 9, 17, 25 August). The size (area) of each blue square is proportional to the sample size for each bin of forecasts, and the grey zones show regions where the forecasts contribute positively to the Brier Skill Scores. Hindcasts have not been smoothed.

variability by 5–25% (against a climatological forecast strategy) for much of the Northern Territory and Queensland. More specifically, the calibrated product shows the greatest improvement over central Australia and the western Lake Eyre Basin, both relative to median and tercile probabilities, when compared to the raw and bias-corrected hindcasts. The calibrated product also dramatically improves the over-prediction bias seen in the raw and bias-corrected hindcasts (Fig. 10). There are two reasons why bias correction does not produce more skilful predictions. Firstly, the raw hindcasts are overly wet across much of central Australia, compared to observations (Fig. S1 in Supplementary Material), and as rainfall can only be positive, the bias correction does not entirely remove the wet bias due to this constraint. As such, the earlier-than-observed onset bias still persists (e.g., Fig. 6). Secondly, for regions drier than observations, such as eastern Queensland, the bias correction process may fix the mean bias, however this invariably increases the frequency of drizzle days (daily rainfall < 1 mm). In these cases, the bias corrected hindcasts produces earlier onsets, as reflected in an example over eastern Queensland for one hindcast member in 1990 (e.g., Fig. S3 in Supplementary Material). Hence, calibration is a more effective method of bias removal due to the quantile–quantile matching approach correcting for the tails of the distributions.

4.1. The 2019/2020 onset forecast

It is for the reasons outlined above that the calibrated product from ACCESS-S1 is used for real-time onset prediction of the NRO. The first operational forecasts using ACCESS-S1, for the 2019/2020 wet season, were widely featuring a low chance (20–30%) of early onset for large portions of central and northeastern Australia (Fig. 12a). The outlook is referenced against the 1960–2012 long-term median and based on a 99-simulation ensemble from 23-25 August 2019 initialisations (the June forecast also showed very similar probabilities). Shown in Fig. 12b is the observed NRO date anomaly map issued on the 26 May 2020, where coloured regions indicate where the observed NRO anomaly was late (brown) or early (green). This shows that the first operational forecast from ACCESS-S1 was widely successful, picking up deficiencies everywhere aside from east Arnhem Land and central southern Queensland. These latter locations saw isolated rainfall activity over a 3-day period between 30 October to 1 November, but very little follow-up rainfall for the remainder of November.

4.2. Comparison of ACCESS-S1 to POAMA2

Finally, we come to the question of whether there is a substantial

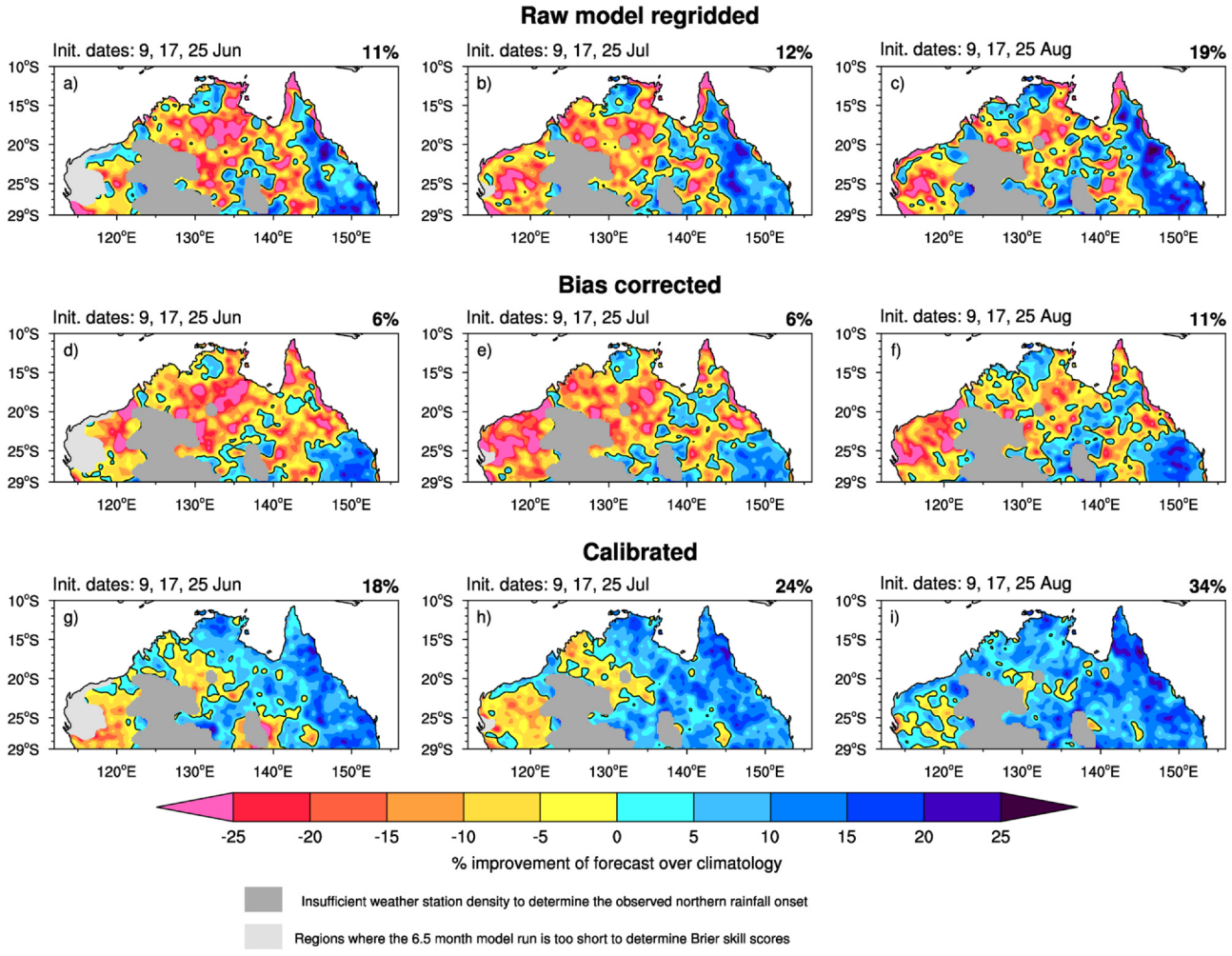

Fig. 11. As in Fig. 9 but for the tercile probability hindcasts.

improvement in ACCESS-S1 over POAMA2 with respect to the NRO prediction, even though our study did not quantify the skill improvements or lack thereof in ACCESS-S1 relative to POAMA2. It is difficult to compare like-for-like, as the atmospheric model resolution of POAMA2 is coarser than ACCESS-S1 (~250 km versus 60 km), the hindcast period is longer at 1960–2010 (compared to 1990–2012), there are more ensemble members per initialisation date (30 to 33 versus 11) meaning initialisation dates do not need to be combined, and the hindcasts are run out to 9 months as opposed to 6.5 months in ACCESS-S1. Putting those differences aside, it is clear from the raw regridded hindcasts, that ACCESS-S1 generally performs better than POAMA2 at capturing the spatial patterns of climatogical median onsets over most of the far northern Australia, including the Top End and Cape York (comparing Fig. 3a of Drosdowsky and Wheeler (2014) with our Fig. 5b).

The Brier Skill scores are more comparable between the ACCESS-S1 calibrated hindcasts and the multi-week POAMA2 hindcasts (run for 1981–2011) than for the raw ACCESS-S1 hindcasts, which again justifies the benefit of calibration. Adding to this, we know that ACCESS-S1 is already considered an improvement in its prediction of the mean-state temperature and precipitation on a sub-seasonal time-scale, yet it does not display enhanced skill over the seasonal time-scale (Hudson et al., 2017a; Lim et al., 2016). A positive aspect of ACCESS-S1's hindcast probabilities are that they are determined with respect to the observed climatological median and not with respect to the model climatology as with POAMA2 (Drosdowsky and Wheeler, 2014). This provides further evidence that ACCESS-S1 is an improvement over POAMA2. The next generation system, ACCESS-S2, includes the BOM's own data assimilation scheme as well as longer hindcasts. This will allow for a more comprehensive analysis of the NRO including an assessment of the skill in capturing longer-term trends.

5. Final remarks

The benefits of both providing a NRO forecast product, and doing so using ACCESS-S1 are clear. The NRO is simple to understand, easy to interpret and well predicted from austral winter onward making it suitable for the northern Australian livestock industry, as well sectors like cropping, infrastructure and telecommunications in terms of planning for the commencement of the wet season. Through its improvement in ENSO prediction and calibrating raw hindcasts to account for model biases, ACCESS-S1 is more skilful in its NRO prediction than Australia's previous dynamical seasonal model. The ongoing need for improved climate services and climate literacy throughout northern Australia is driving research and development into targeted forecasts products, particularly specific to the northern livestock sector, which can provide a significant economic benefit (Cobon et al., 2020). With the Bureau now providing fortnightly and intra-seasonal forecasts (including measures of skill), the next step forward in wet season forecasting is to provide a tailored metric that describes high-frequency rainfall events or 'bursts' as the wet season progresses. Graziers are dependent on knowing when and where these multi-day rainfall events will occur, so as to allow themselves sufficient time to make cost-effective decisions on the logistics of mustering cattle to new pasture

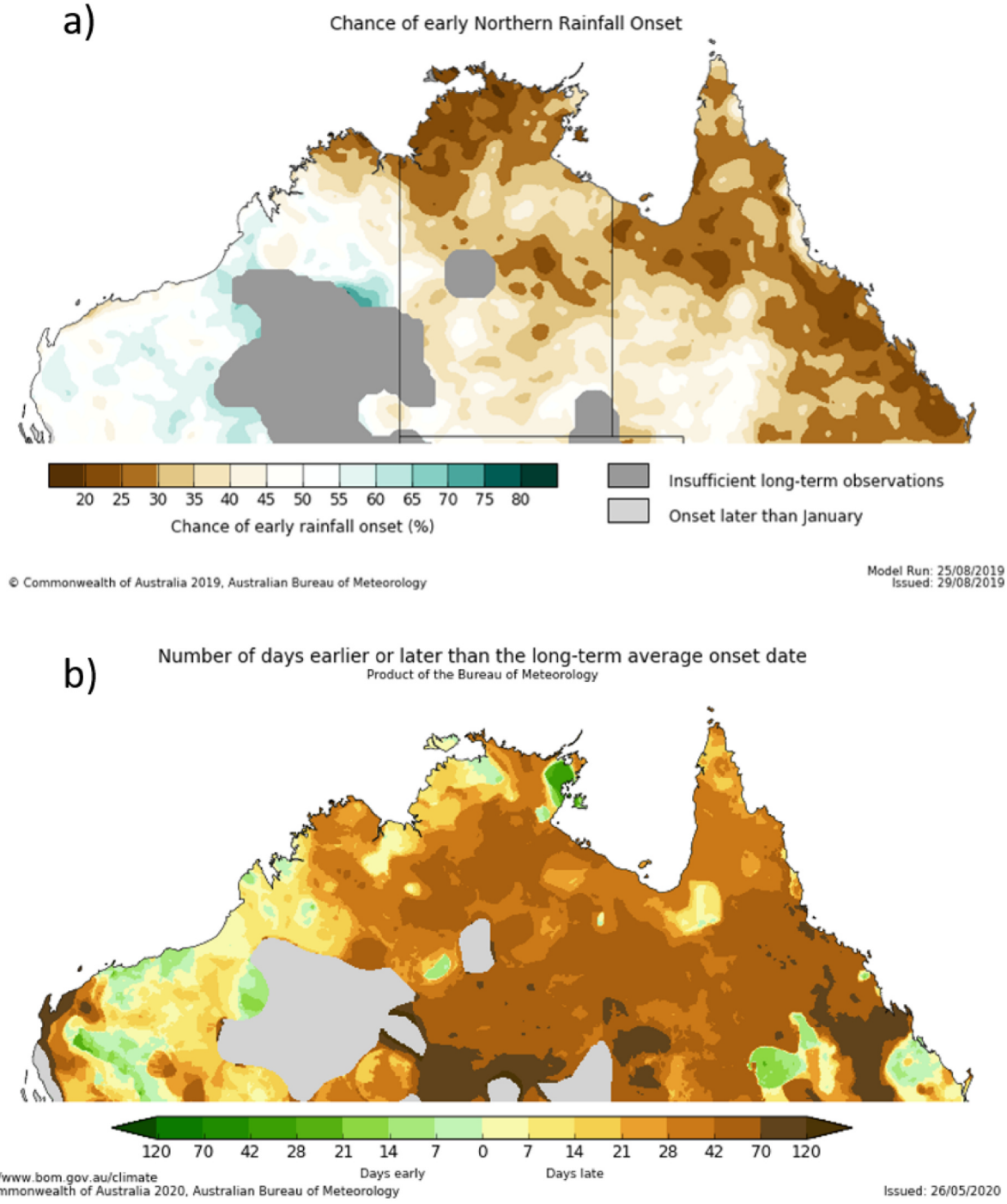

Fig. 12. Verification of the first operational forecast of the NRO by ACCESS-S1 for the wet season of 2019/2020. Shown are (a) the chance of earlier than long-term median onset from ACCESS-S1 based on an 99-model ensemble initialised on the 23–25 August 2019; and (b) the observed NRO date anomaly for 2019/2020, issued on the 26 May 2020. The long-term median onset for the anomaly map is calculated over 1981–2010.

growth locations (McCown, 1981; McCown et al., 1981; Mollah and Cook, 1996; Balston and English, 2009; McRae, 2013), or in the case of extremes (Cowan et al., 2019), implement mitigation measures to protect livestock, or delay transportation. The BOM is currently developing prototype forecast products related to monsoon burst frequency, which, in the near-future, will be an additional climate service to the northern Australian cattle producers.

Declaration of Competing Interest

The authors declare that they have no known competing financial interests or personal relationships that could have appeared to influence the work reported in this paper.

Acknowledgments

This work is funded by Meat and Livestock Australia (MLA), the Queensland Government through the Drought and Climate Adaptation Program, and University of Southern Queensland through the Northern Australian Climate Program (NACP). We particularly thank the ACCESS-S seasonal prediction team, particularly those who develop and maintain the prototype products, including Catherine de Burgh-Day,

Griffith Young, Hailin Yan, Harley Dallafiore and Debra Hudson. Thank-you to Peter van Rensch for his inciteful review and discussions. Real-time forecasts of the NRO can be found here, with archives from POAMA2 located here.

Appendix A. Supplementary data

Supplementary data associated with this article can be found, in the online version, at https://doi.org/10.1016/j.cliser.2020.100182.

References

Balston, J., English, B., 2009. Defining and predicting the 'break of the season' for north-east Queensland grazing areas. Rangeland J. 31 (1), 151–159. https://doi.org/10.1071/RJ08054.

Berry, G.J., Reeder, M.J., 2016. The dynamics of Australian monsoon bursts. J. Atmos. Sci. 73, 55–59. https://doi.org/10.1175/JAS-D-15-0071.1.

Brown, J.N., Ash, A., MacLeod, N., McIntosh, P., 2019. Diagnosing the weather and climate features that influence pasture growth in Northern Australia. Clim. Risk Manage. 24, 1–12. https://doi.org/10.1016/j.crm.2019.01.003.

Cobon, D.H., Darbyshire, R., Crean, J., Kodur, S., Simpson, M., Jarvis, C., 2020. Valuing seasonal climate forecasts in the Northern Australia beef industry. Weather Clim. Soc. 12 (1), 3–14. https://doi.org/10.1175/WCAS-D-19-0018.1.

Cobon, D.H., Stone, G., Carter, J., McKeon, G., Zhang, B., Heidemann, H., 2020. Native pastures and beef cattle show a spatially variable response to a changing climate in Queensland, Australia. Eur. J. Agron. 114 (126), 002. https://doi.org/10.1016/j.eja.2020.126002.

Cowan, T., Wheeler, M.C., Alves, O., Narsey, S., de Burgh-Day, C., Griffiths, M., Jarvis, C., Cobon, D.H., Hawcroft, M.K., 2019. Forecasting the extreme rainfall, low temperatures, and strong winds associated with the northern Queensland floods of February 2019. Weather Clim. Extremes 26 (100), 232. https://doi.org/10.1016/j.wace.2019.100232.

de Burgh-Day, C.O., Spillman, C.M., Stevens, C., Alves, O., Rickard, G., 2019. Predicting seasonal ocean variability around New Zealand using a coupled ocean-atmosphere model. NZ J. Mar. Freshwat. Res. 53 (2), 201–221. https://doi.org/10.1080/00288330.2018.1538052.

Dee, D.P., Uppala, S.M., Simmons, A.J., Berrisford, P., Poli, P., Kobayashi, S., Andrae, U., Balmaseda, M.A., Balsamo, G., Bauer, P., Bechtold, P., Beljaars, A.C.M., Van de Berg, L., Bidlot, J., Bormann, N., Delsol, C., Dragani, R., Fuentes, M., Geer, A.J., Haimberger, L., Healy, S.B., Hersbach, H., Holm, E.V., Isaksen, L., Kallberg, P., Kohler, M., Matricardi, M., McNally, A.P., Monge-Sanz, B.M., Morcrette, J.J., Park, B.K., Peubey, C., de Rosney, P., Tavolato, C., Thepaut, J.N., Vitart, F., 2011. The ERA-Interim reanalysis: configuration and performance of the data assimilation system. Q. J. R. Meteorol. Soc. 137, 553–597. https://doi.org/10.1002/qj.828.

Drosdowsky, W., Wheeler, M.C., 2014. Predicting the onset of the north australian wet season with the POAMA dynamical prediction system. Weather Forecasting 29 (1), 150–161. https://doi.org/10.1175/WAF-D-13-00091.1.

Hudson, D., Alves, A., Hendon, H.H., Lim, E.-P., Liu, G., Luo, J.-J., MacLachlan, C., Marshall, A.G., Shi, L., Wang, G., Wedd, R., Young, G., Zhao, M., Zhou, X., 2017a. ACCESS-S1: The new Bureau of Meteorology multi-week to seasonal prediction system. J. Southern Hemisphere Earth Syst. Sci. 67 (3), 132–159 10.22499/3.6703.001.

Hudson, D., Shi, L., Alves, O., Zhao, M., Hendon, H., Young, G., 2017b. Performance of ACCESS-S1 for key horticultural regions. In: Tech. Rep. No. 20 Bureau of Meteorology Australia.

Hudson, D., Marshall, A.G., Yin, Y., Alves, O., Hendon, H.H., 2013. Improving intraseasonal prediction with a new ensemble generation strategy. Mon. Weather Rev. 141 (12), 4429–4449. https://doi.org/10.1175/MWR-D-13-00059.1.

Jeon, S., Paciorek, C.J., Wehner, M.F., 2016. Quantile-based bias correction and uncertainty quantification of extreme event attribution statements. Weather Clim. Extremes 12, 24–32. https://doi.org/10.1016/j.wace.2016.02.001.

Jones, D.A., Wang, W., Fawcett, R., 2009. High-quality spatial climate data-sets for Australia. Australian Meteorol. Oceanogr. J. 58, 233–248.

King, A.D., Hudson, D., Lim, E.-P., Marshall, A.G., Hendon, H.H., Lane, T.P., Alves, O., 2020. Sub-seasonal to seasonal prediction of rainfall extremes in Australia. Q. J. R. Meteorol. Soc. 1–22. https://doi.org/10.1002/qj.3789.

King, A., Hudson, D., Lim, E.-P., Marshall, A., Hendon, H.H., Lane, T., Henley, B., Cowan, T., Alves, O., 2019. Challenges in assessing skill of seasonal forecasts in Australia. Forecasting for the Future: new science for improved weather, water, ocean and climate services. Bureau Res. Report 40.

Lim, E.-P., Hendon, H., Hudson, D., Zhao, M., Shi, L., Alves, O., Young, G., 2016. Evaluation of the ACCESS-S1 hindcasts for prediction of Victorian seasonal rainfall. Bureau Res. Report 19.

Lisonbee, J., Ribbe, J., Wheeler, M., 2019. Defining the north Australian monsoon onset: a systematic review. Progr. Phys. Geogr.: Earth Environ. https://doi.org/10.1177/0309133319881107.

Lo, F., Wheeler, M.C., Meinke, H., Donald, A., 2007. Probabilistic forecasts of the onset of the north Australian wet season. Mon. Weather Rev. 135 (10), 3506–3520. https://doi.org/10.1175/MWR3473.1.

MacLachlan, C., Arribas, A., Peterson, K.A., Maidens, A., Fereday, D., Scaife, A.A., Gordon, M., Vellinga, M., Williams, A., Comer, R.E., Camp, J., Xavier, P., Madec, G., 2015. Global Seasonal forecast system version 5 (GloSea5): a high-resolution seasonal forecast system. Q. J. R. Meteorol. Soc. 5, 1072–1084. https://doi.org/10.1002/qj.2396.

Marshall, A., Hendon, H., 2019. Multi-week prediction of the Madden-Julian oscillation with ACCESS-S1. Clim. Dyn. 52, 2513–2528. https://doi.org/10.1007/s00382-018-4272-6.

McBride, J.L., 1987. The Australian summer monsoon. In: Chang, C.P., Krishnamurti, T.N. (Eds.), Reviews of Monsoon Meteorolog. Oxford University Press, Oxford, UK, pp. 203–231.

McCown, R., Gillard, P., Winks, L., Williams, W.T., 1981. The climatic potential for beef cattle production in tropical Australia: Part II–Liveweight change in relation to agroclimatic variables. Agric. Syst. 7, 1–10. https://doi.org/10.1016/0308-521X(81)90024-X.

McCown, R.L., 1981. The climatic potential for beef cattle production in tropical Australia: Part I – Simulating the annual cycle of liveweight change. Agric. Syst. 135, 303–317. https://doi.org/10.1016/0308-521X(81)90065-2.

McRae, D., 2013: What is my 'green day'? Queensland Country Life, published 26 December.

Moise, A., Smith, I., Brown, J.R., Colman, R., Narsey, S., 2019. Observed and projected intra-seasonal variability of Australian monsoon rainfall. Int. J. Climatol. https://doi.org/10.1002/joc.6334. in press.

Mollah, W.S., Cook, I.M., 1996. Rainfall variability and agriculture in the semi-arid tropics – The Northern Territory, Australia. Agric. For. Meteorol. 79, 39–60. https://doi.org/10.1016/0168-1923(95)02267-8.

Narsey, S., Reeder, M.J., Jakob, C., Ackerley, D., 2018. An Evaluation of Northern Australian Wet Season Rainfall Bursts in CMIP5 Models. J. Clim. 31 (19), 7789–7802. https://doi.org/10.1175/JCLI-D-17-0637.1.

Nicholls, N., 1984. A system for predicting the onset of the North Australian wet-season. J. Climatol. 4, 425–435.

Nicholls, N., McBride, J.L., Ormerod, R.J., 1982. On predicting the onset of the Australian wet season at Darwin. Mon. Weather Rev. 110, 14–17.

Pope, M., Jakob, C., Reeder, M.J., 2009. Regimes of the north Australian wet season. J. Climate 22, 6699–6715. https://doi.org/10.1175/2009JCLI3057.1.

Risbey, J.S., Pook, M.J., McIntosh, P.C., Wheeler, M.C., Hendon, H.H., 2009. On the remote drivers of rainfall variability in Australia. Mon. Weather Rev. 137, 3233–3253. https://doi.org/10.1175/2009MWR2861.1.

Shi, L., Hudson, D., Alves, O., Young, G., MacLachlan, C., 2016. Comparison of GloSea5-GC2 skill with POAMA-2 for key horticultural regions. Tech. Rep. No. 13, Bureau of Meteorology Australia.

Smith, G., Spillman, C., 2019. New high-resolution sea surface temperature forecasts for coral reef management on the Great Barrier Reef. Coral Reefs 38, 1039–1056. https://doi.org/10.1007/s00338-019-01829-1.

Troup, A.J., 1961. Variations in upper tropospheric flow associated with the onset of the Australian summer monsoon. Ind. J. Meteor. Geophys. 12, 217–230.

Walters, D., Boutle, I., Brooks, M., Melvin, T., Stratton, R., Vosper, S., Wells, H., Williams, K., Wood, N., Allen, T., Bushell, A., Copsey, D., Earnshaw, P., Edwards, J., Gross, M., Hardiman, S., Harris, C., Heming, J., Klingaman, N., Levine, R., Manners, J., Martin, G., Milton, S., Mittermaier, M., Morcrette, C., Riddick, T., Roberts, M., Sanchez, C., Selwood, P., Stirling, A., Smith, C., Suri, D., Tennant, W., Vidale, P.L., Wilkinson, J., Willett, M., Woolnough, S., Xavier, P., 2017. The Met Office Unified Model Global Atmosphere 6.0/6.1 and JULES Global Land 6.0/6.1 configurations. Geosci. Model Develop. 10 (4), 1487–1520. https://doi.org/10.5194/gmd-10-1487-2017.